Newly generated neurons in the amygdala and adjoining cortex of adult primates

Patrick J. Bernier*, Andréanne Bédard*, Jonathan Vinet, Martin Lévesque, and André Parent†

Centre de Recherche Université Laval-Robert-Giffard, 2601, Chemin de la Canardière, Local F-6500, Beauport, QC, Canada G1J 2G3

Communicated by Charles G. Gross, Princeton University, Princeton, NJ, July 8, 2002 (received for review May 10, 2002)

The subventricular zone remains mitotically active throughout life in rodents. Studies with tritiated thymidine, which is incorporated into the DNA of mitotic cells, have revealed that the rodent subventricular zone produces neuroblasts that migrate toward the olfactory bulb along the rostral migratory stream. A similar migratory stream has been documented in monkeys by using the thymidine analogue BrdUrd. The same approach showed that neurogenesis occurred in the dentate gyrus of adult primates, including humans. In the present study, experiments combining injections of BrdUrd and the dye 1,1′-dioctadecyl-3,3,3′,3′-tetramethylindo-carbocyanine, with the immunostaining for molecular markers of neurogenesis (polysialylated neural cell adhesion molecule, β-tubulin-III, collapsin response mediator protein-4, neuronal nuclear protein) in New World (*Saimiri sciureus*) and Old World (*Macaca fascicularis*) monkeys have revealed that new neurons are produced in the amygdala, piriform cortex, and adjoining inferior temporal cortex in adult primates. These newborn neurons expressed the antiapoptotic protein Bcl-2 and formed a more-or-less continuous pathway that extended from the tip of the temporal ventricular horn to the deep portion of the temporal lobe. The production of newborn neurons in the amygdala, piriform cortex, and inferior temporal cortex seems to parallel the continuing addition of neurons in the olfactory bulb. These two concomitant phenomena may ensure structural stability and functional plasticity to the primate olfactory system and temporal lobe.

Neurogenesis is known to occur throughout life in specific areas of the mammalian brain, principally the dentate gyrus of the hippocampus and the subventricular zone (SVZ) that lines the lateral ventricles (1, 2). Adult SVZ produces neuroblasts that migrate tangentially toward the olfactory bulb along the so-called rostral migratory stream (RMS) (3, 4). Tangential migration is rare in embryonic brain development, but more than 50% of neurons generated prenatally in rodents seem to migrate tangentially for a certain distance before their final radial implantation (5). Therefore, it can be expected that a majority of neurons produced in mature brain would follow a tangential route to reach implantation level. In any event, the fact that migrating chains have been observed along the entire lateral ventricle system (6, 7) raises the possibility of the existence of migratory streams other than the RMS. Indeed, evidence shows that new neurons are produced in various neocortical regions in monkeys (8), but these cells seem to be transient (9).

The present investigation was designed to study newly generated neurons in the deep portion of the temporal lobe of adult monkeys by using the thymidine analogue BrdUrd, which is incorporated into DNA of mitotic cells, combined with immunostaining for highly reliable molecular markers of newborn neurons.

Experimental Procedures

Preparation of the Animals and BrdUrd Injections. Nine adult (3–6 years of age) squirrel monkeys (*Saimiri sciureus*) and four adult (6–12 years of age), cynomolgus monkeys (*Macaca fascicularis*) were used, and all experimental procedures followed the guidelines of the Canadian Council on Animal Care. All cynomolgus monkeys and seven of the nine squirrel monkeys received i.v. injections of BrdUrd (Sigma) dissolved in 0.9% NaCl with 0.007 M NaOH, 50 mg/kg body weight. Except for the animal that survived only 1 day after a single BrdUrd injection, the other animals were injected twice a day for 3 days. The four macaques were killed at 1, 7, 14, or 21 days after the last injection. The seven squirrel monkeys that received BrdUrd were killed 21 days (four animals) and 28 days (three animals) after the last injection. They were deeply anesthetized with ketamine/xylazine and perfused transcardially with a saline solution, followed by 4% paraformaldehyde in phosphate buffer (PB, 0.1 M, pH 7.4). The brains were washed with 10% sucrose solution in PB, removed from the skull, and placed in a cryoprotective solution (30% sucrose in PB) until immersion. They were then sectioned along the sagittal or coronal planes at 40 μm with a freezing microtome.

DiI Injections. Three squirrel monkeys, including one that was injected with BrdUrd, received single intraventricular injections of 80 μl of 1,1′-dioctadecyl-3,3,3′,3′-tetramethylindo-carbocyanine ($SP\text{-}DiIC_{18}$, or DiI, Molecular Probes) dissolved in dimethylformamide (VWR Scientific). The dye was injected with a Hamilton syringe in the left lateral ventricle by using the stereotaxic coordinates of the atlas of Emmers and Akert (10). The animals were perfused 3 weeks after the injection.

Immunohistochemistry. BrdUrd was detected according to a standard method described in detail (11). In brief, the sections were blocked for 30 min in a PBS solution (0.1 M, pH 7.4) containing 0.1% Triton X-100 (Sigma) and 2% normal horse serum or normal goat serum. They were incubated overnight at 4°C in the same solution containing mouse anti-BrdUrd (Sigma; 1:1,000) or rat anti-BrdUrd (Accurate Scientific, Westbury, NY; 1:200).

Before immunostaining for polysialylated neural cell adhesion molecule (PSA-NCAM), class III β-tubulin (TuJ1), collapsin response mediator protein-4 (TUC-4), or antiapoptotic Bcl-2 protein, the sections were placed in a solution of hydrogen peroxide (3%) for 30 min at room temperature. They were then blocked for 30 min in a PBS solution containing 0.1% Triton X-100 and 2% normal serum. The sections were then washed in PBS and incubated overnight at 4°C (48 h for Bcl-2 and room temperature incubation for TUC-4) in a solution containing either mouse anti-Bcl-2 (Roche Molecular Biochemicals, clone 124; 1:50), mouse anti-TuJ1 (a generous gift of A. Frankfurter, 1:4,000), rabbit anti-TUC-4 (Chemicon; 1:500), or mouse anti-PSA-NCAM (anti-MEN-B; a generous gift from G. Rougon; 1:200). The sections were then incubated for 1 h at room temperature in 0.4% biotinylated secondary antibody (Vector Laboratories). After several washings in PB, the sections were reincubated for 1 h at room temperature in 2% avidin–biotin

Abbreviations: NeuN, neuronal nuclear protein; PSA-NCAM, polysialylated neural cell adhesion molecule; SVZ, subventricular zone; tLV, temporal horn of lateral ventricles; TS, temporal stream; TuJ1, β-tubulin-III; TUC-4, collapsin response mediator protein-4; GFAP, glial fibrillary acidic protein; MAP-2, microtubule-associated protein-2; RMS, rostral migratory stream; DiI, 1,1′-dioctadecyl-3,3,3′,3′-tetramethylindo-carbocyanine.

*P.J.B. and A.B. contributed equally to this work.

†To whom reprint requests should be addressed. E-mail: andre.parent@anm.ulaval.ca.

 www.pnas.org/cgi/doi/10.1073/pnas.172403999

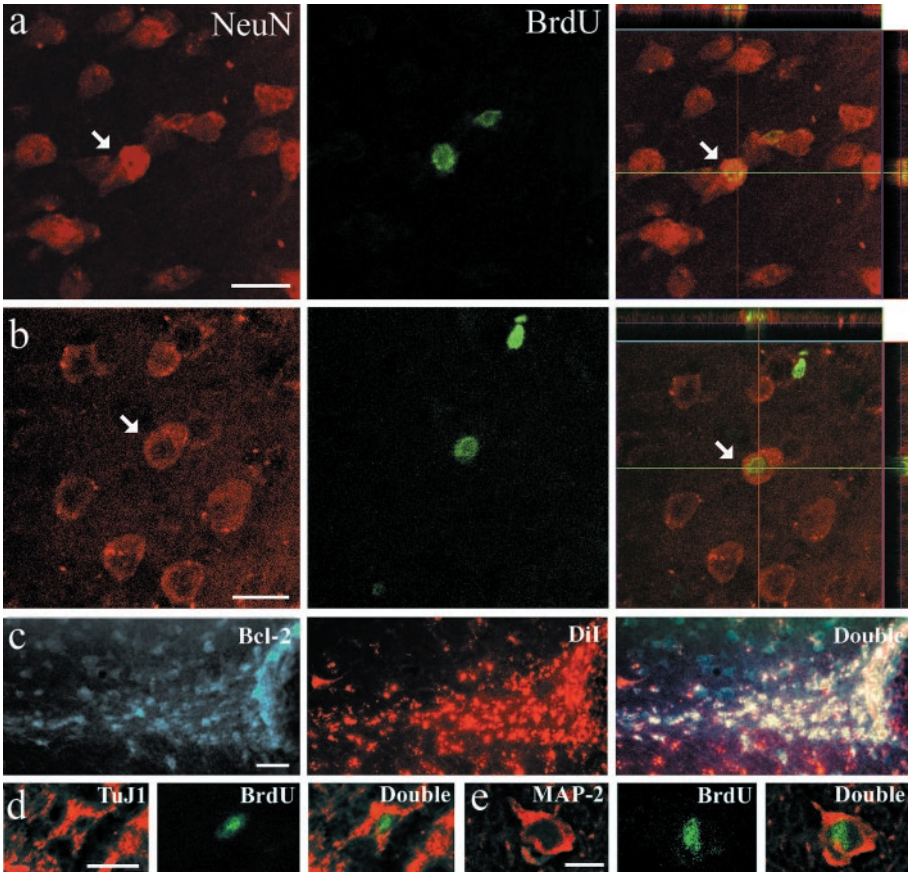

Fig. 1. Colocalization of neurogenesis markers in the rostral portion of the temporal lobe of squirrel monkeys that were killed 21 and 28 days after the last BrdUrd injection. Examples of a cell in the amygdala (*a*) and piriform cortex (*b*) that have incorporated BrdUrd (green) and also express NeuN (red). The right side shows reconstructed orthogonal images of the same NeuN+/BrdUrd+ cells, which are viewed from the sides in both *x*–*z* (top) and *y*–*z* (right) planes. (*c*) Cells in TS are colabeled for DiI (red) and for Bcl-2 (green). (*d*) TuJ1+/BrdUrd+ cell in TS and (*e*) MAP-2+/BrdUrd+ cell in amygdala. The various neuronal markers are stained in red, whereas BrdUrd is in green. [Bars = 25 μm (*a* and *b*), 100 μm (*c*), 15 μm (*d* and *e*).]

complex (Vector Laboratories), and the immunoprecipitate was revealed with 3,3′-diaminobenzidine (Sigma) as the chromogen, except for Bcl-2 that was revealed with nickel-intensified 3,3′-diaminobenzidine (Sigma). Sections incubated without the primary antibody remained virtually free of immunostaining and served as controls.

Immunofluorescence. Coexpression of the above-mentioned molecular markers was examined with a double-immunofluorescence approach. After BrdUrd revelation with Alexa-488 goat anti-rat IgG (Molecular Probes; 1:200), the sections were reincubated with either mouse anti-TuJ1, rabbit anti-glial fibrillary acidic protein (GFAP) (Sigma, 1:80), mouse anti-microtubule-associated protein-2 (MAP-2) (Sigma, 1:500) or mouse anti-neuronal nuclear protein (NeuN) (Chemicon; 1:100). The second primary antibody was revealed with an Alexa-568 goat anti-mouse or goat anti-rabbit IgG (Molecular Probes; 1:200). Sections incubated without the primary antibodies remain unstained and served as controls. Fluorescent signals were imaged by using a Zeiss LSM 510 confocal laser-scanning microscope. To ensure that a cell that seemed doubled-labeled was not, instead, two closely apposed, single-labeled cells (12), a *Z*-stack analysis was performed at 1-μm intervals. The emission signals of Alexa 488 and 568 were assigned to green and red channels, respectively.

Results

BrdUrd Labeling. The present analysis was limited to the rostral portion of the temporal lobe, that is, the amygdala and its immediate surroundings. Because it has already been the subject of several investigations, the hippocampus was not analyzed here. In squirrel monkeys, numerous BrdUrd-positive (+) nuclei occurred along a more-or-less continuous pathway that extended from the rostral tip of the ventral portion of the temporal horn of the lateral ventricle (tLV) to the amygdala and piriform cortex. The narrow band of BrdUrd+ nuclei that links the tLV with the dorsal aspect of the amygdala will be referred to here as the temporal stream (TS). Many of the BrdUrd+ nuclei that were scattered along the TS displayed an elongated shape and most of them had their longest axis oriented parallel to the main axis of the TS. As they approached the amygdala and piriform cortex, however, the elongated BrdUrd+ nuclei were oriented in all directions. The BrdUrd+ nuclei abounded particularly within the basolateral sector of the amygdala, whereas they tended to form clusters within the piriform cortex. A few BrdUrd+ nuclei were also disclosed within the deep layers of the inferior temporal cortex.

The neuronal nature of many BrdUrd+ cells encountered in the amygdala, the surrounding piriform cortex, and the inferior temporal cortex was ensured by the fact these cells also expressed immunoreactivity for NeuN or MAP-2, two markers of mature neurons (13, 14) or TuJ1, a marker of early committed neurons (15) (Figs. 1 and 2). An estimate of the rate of production of various cell types in primate temporal lobe was obtained by evaluating the percentage of the different types of doubly labeled cells in the TS and in the specific sector of the amygdala and piriform cortex (dotted lines in Fig. 5*e*) in the three squirrel

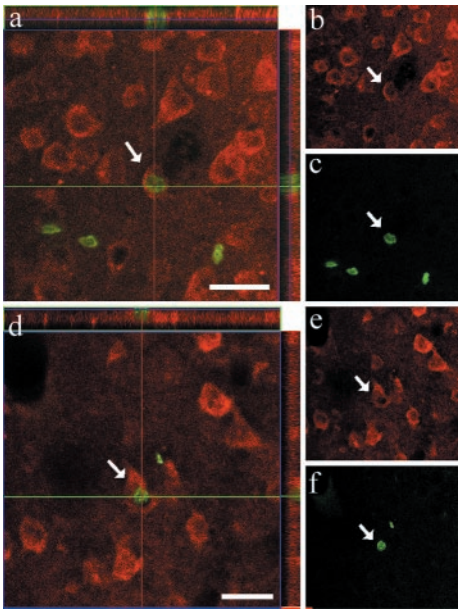

Fig. 2. (*a–f*) Two BrdUrd+/NeuN+ cells encountered in the inferior temporal cortex of an adult squirrel monkey that have incorporated BrdUrd (green) and also express NeuN (red). This animal was killed 28 days after the last BrdUrd injection. (*Left*) Orthogonal views. (*Right*) Separate labeling views. (Bars in *a* and *d* = 25 μm.)

monkeys that survived 28 days after BrdUrd injections (Fig. 3). The number of BrdUrd+ cells in the TS, amygdala, and piriform cortex was compared with that of cells labeled for both BrdUrd and one of the following markers: TuJ1, MAP-2, TUC-4 (a marker of postmitotic granule neuroblasts; refs. 16 and 17),

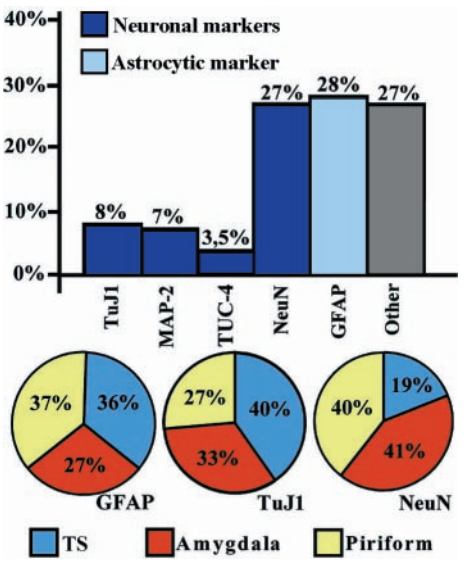

Fig. 3. Bar and circle histograms depicting the relative proportion of the different types of cells that have incorporated BrdUrd in the TS and the rostral sector of the temporal lobe (see Fig. 5*e* for exact delimitation) of adult squirrel monkeys that were killed 28 days after the last BrdUrd injection. The bar histogram shows the percentage of neuronal (MAP-2, NeuN), immature neuronal (TuJ1, TUC-4) or astrocytic (GFAP) markers relative to the total number of BrdUrd-labeled nuclei. The column named 'Other' refers to the percentage of cells that do not express NeuN or GFAP. The circle diagrams illustrate the proportion of BrdUrd+ cells that were also labeled for GFAP, TuJ1, and NeuN in the TS (blue), amygdala (yellow), and piriform cortex (red).

NeuN, and GFAP. An average of 7.7 BrdUrd+ cells per 40-μm-thick section was found in the TS, compared with 13.4 and 14.3 BrdUrd+ cells in the amygdala and piriform cortex, respectively. Because stringent criteria were applied for the identification of doubly labeled cell, the real number of newly generated cells may in fact be higher than what is reported here.

Markers of Newborn Neurons. Beside its well-known antiapoptotic property, Bcl-2 is also known to accelerate maturation of neuroblasts (18, 19) and regulate neuronal differentiation (20). We have previously reported high levels of Bcl-2 in zones that are now known to be sites of postnatal neurogenesis in adult monkeys. We also described a thick band under the amygdala that was intensely stained for Bcl-2 and from which chains of cells seemed to invade the amygdaloid complex (21). Moreover, we recently colocalized Bcl-2 with nestin, PSA-NCAM, and β-tubulin-III in cells of human SVZ (6). These findings support the idea that Bcl-2 is closely related to neurogenesis.

By virtue of its intense expression in every adult neurogenesis area, which contrasts with the very low expression of this protein in most other adult brain areas, Bcl-2 can serve as a reliable marker of neurogenesis in the adult primate brain. Furthermore, because it is expressed during the entire length of differentiation and maturation phases, Bcl-2 allows the detection of larger populations of newborn cells *in situ*. Numerous cells expressing Bcl-2 were scattered throughout the TS. They were small, round to oval, with only one or two processes, and formed typical chains or clusters scattered all along the TS. As the pathway reached the piriform cortex, the Bcl-2+ cells appeared as tightly packed clusters (Fig. 4 *a* and *b*).

In squirrel monkeys, PSA-NCAM immunostaining delineated the same pathway as the one visualized after Bcl-2 immunostaining or DiI injection (see below). The PSA-NCAM+ cells were scattered all along the TS, but appeared in the form of clusters of various sizes in the piriform cortex (Fig. 4*c*). Many chains of neuroblasts in the TS expressed TuJ1 (Fig. 4*d*). Some of these TuJ1+ neurons seemed to have been newly generated because BrdUrd+/TuJ1+ cells were detected all along the TS (Fig. 1*d*).

The early expression of TUC-4 and its relative abundance in newborn neurons, as well as the restriction in its expression to the period of initial neuronal differentiation have led to use this protein as another specific marker of recently generated neurons in the adult brain. The TS in squirrel monkeys was found to stain for TUC-4 (Fig. 4*e*). A thin array of TUC-4+ cells extended from the tLV to the subamygdalaloid region. Furthermore, small clusters of TUC-4+ cells with thick fibers fascicles oriented toward the TS were seen in piriform cortex (Fig. 4 *f–g*).

Evidence for Cell Migration. The proliferating cells in the temporal lobe of squirrel and cynomolgus monkeys were exposed to BrdUrd for about 12 h during 3 consecutive days in an attempt to delineate a possible migratory stream from the SVZ to the amygdala. However, because the SVZ proliferation rate may be slower in primates than in rodents and because many labeled cells die before reaching their final destination (22), it is difficult to follow a sufficiently large number of BrdUrd+ migrants and hence to identify putative migratory streams with BrdUrd labeling alone. Thus, we used DiI, a highly lipophilic dye, to delineate these putative pathways better. When DiI enters living cell membranes, it becomes entrapped and cannot be transferred from one cell to another. In squirrel monkeys, a cohort of DiI+ cells could be traced from the tLV to the amygdala and piriform cortex, thus forming a continuous pathway that was identical to the TS identified above on the basis of BrdUrd staining (Fig. 5 *a–c*). Typical chains of DiI+ cells also occurred at the ventral border of the amygdala (Fig. 5*b*).

The data obtained with DiI are only indicative of the existence

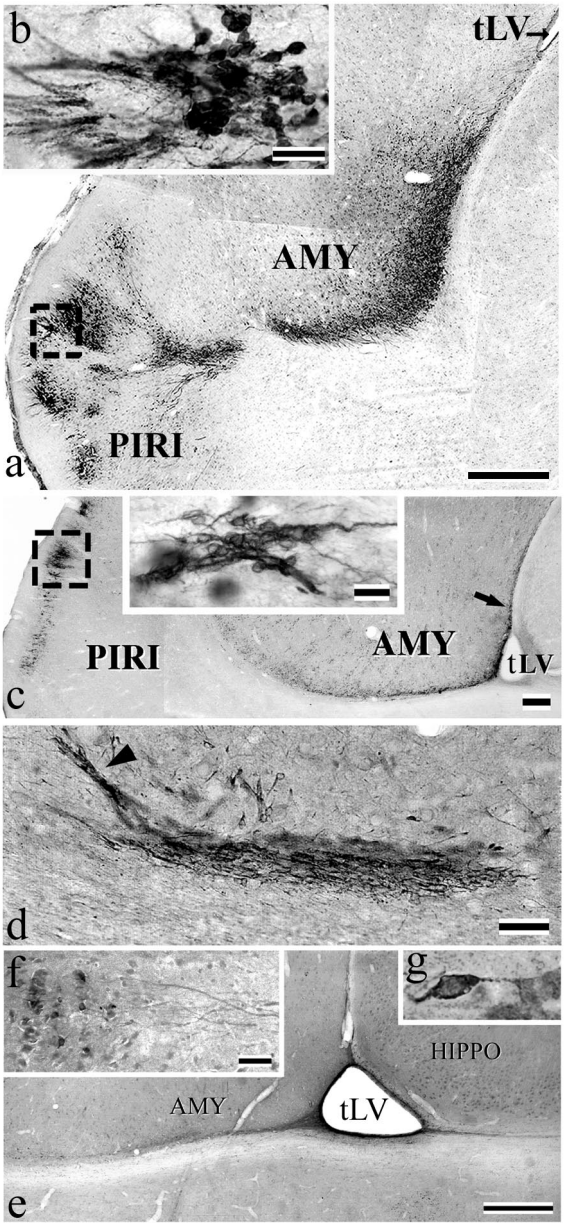

Fig. 4. The squirrel monkey TS as seen on parasagittal sections immunostained with various neurogenesis markers. (*a*) Photomontage showing typical Bcl-2 immunostaining that extends from the tip of the tLV to the amygdala (AMY) and piriform cortex (PIRI). (*b*) High-power view of a cluster of Bcl-2+ cells (box in *a*) in superficial layers of piriform cortex. (*c*) Chains of PSA-NCAM+ cells beneath the amygdala. (*Inset*) A high power view of PSA-NCAM+ chains in piriform cortex (PIRI) (box). (*d*) Chains of β-tubulin-III+ cells in amygdala (see arrow in *c*). Some chains are oriented toward amygdala (arrowhead in *d*). (*e*) Overview of TUC-4 immunoreactivity in the lower part of amygdala (AMY). Note the labeling that emerges form the tip of tLV. (*f*) A typical cluster of TUC-4+ neurons in piriform cortex, from which emerges an array of thick immunopositive fibers. (*g*) High-power view of a TUC-4+ neuron in piriform cortex. [Bars = 500 μm (*a*), 20 μm (*b* and *f*), 250 μm (*c*), 25 μm (*Inset* in *c*), 50 μm (*d*), 1 mm (*e*), and 15 μm (*g*).]

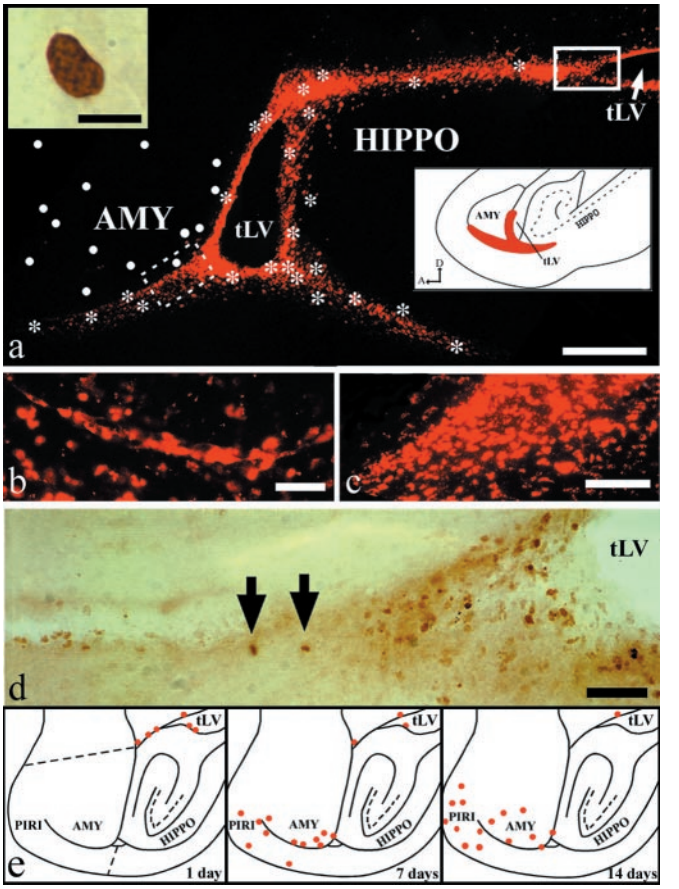

Fig. 5. (*a–d*) DiI-labeling and distribution of BrdUrd+ cells, as seen on a parasagittal section of the temporal lobe of an adult squirrel monkey. (*a*) General view of the typical DiI staining; dots represent BrdUrd+ cells found in amygdala (AMY), whereas asterisks indicate BrdUrd+ cells lying along the DiI+ pathway and its branches. *Inset* (*Upper Left*) displays a high-power view of one typical BrdUrd+ nucleus. For the sake of clarity the numerous BrdUrd+ cells in the hippocampal formation (HIPPO) have not been indicated here. *Inset* (*Lower Right*) depicts the germinal matrix extensions under amygdala (AMY) and hippocampus (HIPPO), as they can be seen on a sagittal section of the temporal lobe of a 26-day-old human embryo (25). (*b* and *c*) A typical chain of DiI+ cells en route to the amygdala (*b*) (dotted line box in *a*) and a pool of DiI+ cells at the tip of the temporal horn of the lateral ventricle (tLV) (*c*). (*d*) BrdUrd+ cells (arrows) that are part of a pool of similar cells at the tip of the tLV (uninterrupted-line box in *a*). (*e*) Plotting of BrdUrd+ nuclei on sagittal sections of adult macaques killed at three different times after the last BrdUrd injection. The red circles indicate BrdUrd+ nuclei that appear at day 1, 7, and 14 after the last BrdUrd injection. For the sake of clarity the numerous BrdUrd+ cells in the hippocampal formation have not been indicated here. The dotted lines in the upper drawing delineate the sector in which quantification was made (see Fig. 3). [Bars = 250 μm (*a*), 5 μm (*Inset* in *a*), 50 μm (*b* and *e*), and 100 μm (*c*).]

of a temporal migratory stream. The visualization of BrdUrd and its colocalization with various molecular markers of neurogenesis in cells located along this DiI-labeled pathway are needed to reach a more definitive conclusion. However, the variation in the pattern of distribution of the BrdUrd+ nuclei in the deep portion of the temporal lobe of cynomolgus monkeys according to the survival time after the last BrdUrd injection is congruent with the idea that the newborn neurons detected in the amygdala and piriform cortex may have migrated from the SVZ that borders the tLV (Fig. 5*e*). In the animal that was allowed to survive only 1 day after a single injection, BrdUrd+ cells were largely confined to the border of the tLV, whereas in the animal that survived 7 days, the majority of BrdUrd+ cells lay along the TS and a smaller number of BrdUrd+ cells occurred in the basolateral portion of the amygdala and in the piriform cortex, including the piriform area, entorhinal cortex, and periamygdaloid cortex. A few BrdUrd+ cells were also detected in the inferior temporal cortex from that time on. Fourteen to 21 days after injection, the BrdUrd+ cells were much more numerous in the amygdala and piriform cortex than in the TS.

Discussion

This study provides evidence for the presence of newly generated neurons in the amygdala and surrounding cortex of adult monkeys. Recently, Gould and colleagues (8) have gathered findings that favor the existence of neurogenesis in specific regions of the neocortex of adult monkeys. New cortical neurons were shown to originate from the SVZ, and it was hypothesized, although not directly demonstrated, that these newborn neurons reach their final destination after migrating radially through the white matter. Although Gould and colleagues (8) did not identify any migratory pathway heading toward the amygdala and surrounding structures, they nevertheless visualized some BrdUrd+ cells in the piriform cortex of monkeys. The latter finding is congruent with the presence of newborn neurons in the deep rostral portion of the temporal lobe in adult primates, as demonstrated here. A distinct migratory stream that corresponds to the rodent RMS has been recently documented in adult primate brain (4, 23). The latter finding suggests that the RMS is a phylogenetically old neurogenetic system that has been retained during mammalian brain evolution.

During rat brain embryogenesis, an extension of the lateral ventricle containing the germinal matrix is present along the growing olfactory bulb. It is generally accepted that this extension becomes the substrate of the postnatal RMS (24). Another germinal matrix extension of the lateral ventricle occurs behind and under the amygdala during human brain development (Fig. *5a Right Inset*) (25). The striking similarity between this extension in embryonic human brain and the TS of adult monkeys described here strengthens the notion of neurogenetic activity in this pathway and its principal recipient structures. Moreover, by analogy with what occurs at the RMS level, it may be presumed that this temporal lobe extension of the germinal matrix serves as a morphological substratum for the adult TS.

Cells doubly labeled for BrdUrd and specific neuronal markers have been detected in the amygdala and piriform cortex of squirrel monkeys, and our quantitative estimates indicate that at least 27% of the newly generated cells that were scattered in the temporal lobe of adult primates differentiate into neurons. Although estimates of newborn neurons were obtained from the sampling of only the rostral part of the temporal lobe, the values nevertheless indicate that the rate of neurogenesis at this level is rather impressive. It is important to note that these findings were gathered from the brain of squirrel monkeys that were raised in colony and housed in a large room that was designed to avoid stress, which is known to inhibit neurogenesis (26), and to provide a maximally enriched environment, a condition that is known to favor neurogenesis (27).

The fact that thick layers of TuJ1+ cells occurred at the TS level and that BrdUrd+ nuclei were scattered all along this pathway suggest that the newborn neurons in the amygdala and piriform cortex might originate from the SVZ surrounding the tLV. Our quantitative immunostaining data indicate that about one-third of the newborn cells had a chemical phenotype that did not correspond to that of newly generated neurons or astrocytes. Most of these cells are likely to be oligodendrocytes, a notion that is congruent with the important role that the SVZ plays in myelinization (28, 29). A significant proportion of this unidentified population may also be undifferentiated stem/precursor cells and/or microglia and phagocytic cells. Further studies with specific molecular markers of immature oligodendrocytes and microglial cells should help in answering these questions.

Also, Bcl-2 labeled virtually all components of the deep portion of the temporal lobe where signs of adult neurogenesis have been detected in the present study. This antiapoptotic protein can thus be considered as a valuable marker of adult neurogenesis in primates.

Although strongly suggestive of the existence of a temporal migratory stream whereby neuroblasts would be conveyed from the SVZ bordering the tLV to the amygdala and its cortical mantle, the data gathered in the present study do not provide a definite proof of this putative migratory phenomenon. For example, the DiI staining observed along the TS may have been the result of a lateral diffusion of this lipophilic dye with time rather than actual cell migration. Focal injections of DiI, or BrdUrd or specific viral vectors, could help solving this issue. On the other hand, the abundance of BrdUrd+ cells in the SVZ adjoining the tLV in early survival periods and the decrease in the number of these cells at the expense of those in the amygdala in longer survival periods support the idea that newborn cells are generated in the SVZ and migrate afterward into the parenchyma of the amygdala. However, the possibility that newly generated cells in the amygdala and surrounding structures result from division of *in situ* progenitor cells cannot be excluded here. Furthermore, longer survival periods after BrdUrd injections are needed to study the fate of the newborn neurons encountered in the amygdala and surrounding cortex. This type of information is essential to know whether the new neurons that populate the amygdala and adjoining cortex in primates are expressed only transiently or if they become fully mature and completely integrated within the neuronal circuitry of the temporal lobe.

In regard to the functional significance of adult neurogenesis in primate temporal lobe, it is worth remembering that parts of both amygdala and piriform cortex receive direct olfactory inputs (30). Hence, the implantation of newly generated neurons into these structures may parallel the continuing addition of new neurons in the olfactory bulb. These two concomitant phenomena might confer stability and plasticity to the olfactory system and temporal lobe. As for the dentate gyrus, the rate of postnatal neurogenesis in the amygdala and adjoining regions of the temporal lobe might be altered by various external conditions, such as stressful events (26). Such a phenomenon could help generate novel hypotheses about the pathogenesis of psychiatric diseases, such as mood/affect disorders and schizophrenia.

Data from lesion, tract-tracing, and electrophysiological studies collectively suggest that the amygdala plays a key role in the adaptation to stressful, fearful, or simply novel situations (31). The implication of this subcortical structure in such complex behavioral responses involves the transmission of sensory information to the amygdala, particularly its lateral portion, where alterations in synaptic transmission are thought to encode the key aspect of the learning (32). Although synaptic plasticity is obviously necessary for learning and memory to occur in the temporal lobe, few data currently support the notion that activity-dependent synaptic plasticity is sufficient to explain the entire complexity of such phenomena (33). On the basis of the data presented here, we postulate that the addition of new neurons significantly enlarges the structural and functional plasticity of the amygdala and, as such, increases its capability to elaborate adequate responses to novel and stressful conditions.

We thank Drs. Geneviève Rougon and Anthony Frankfurter for anti-PSA-NCAM and anti-TuJ1 antibodies. This research was supported by grants from the Canadian Institutes of Health Research.

1. Doetsch, F., Garcia-Verdugo, J. M. & Alvarez-Buylla, A. (1997) *J. Neurosci.* **17,** 5046–5061.
2. Gould, E., Reeves, A. J., Fallah, M., Tanapat, P. & Gross, C. G. (1999) *Proc. Natl. Acad. Sci. USA* **96,** 5263–5267.
3. Lois, C. & Alvarez-Buylla, A. (1994) *Science* **26,** 1145–1148.
4. Kornack, D. R. & Rakic, P. (2001) *Proc. Natl. Acad. Sci. USA* **98,** 4752–4757.
5. O'Rourke, N. A., Chenn, A. & McConnell, S. K. (1997) *Development (Cambridge, U.K.)* **124,** 997–1005.
6. Bernier, P. J., Vinet, J., Cossette, M. & Parent, A. (2000) *Neurosci. Res.* **37,** 67–78.

7. Doestch, F. & Alvarez-Buylla, A. (1996) *Proc. Natl. Acad. Sci. USA* **93,** 14895–14900.
8. Gould, E., Reeves, A. J., Grazianno, M. S. A. & Gross, C. G. (1999) *Science* **286,** 548–552.
9. Gould, E., Vail, N., Wagers, M. & Gross, C. G. (2001) *Proc. Natl. Acad. Sci. USA* **98,** 10910–10917.
10. Emmers, R. & Akert, K. (1963) *A Stereotaxic Atlas of the Brain of the Squirrel Monkey (Saimiri sciureus)* (Univ. of Wisconsin Press, Madison).
11. Bédard, A., Cossette, M., Lévesque, M. & Parent, A. (2002) *Neurosci. Lett.* **328,** 213–216.
12. Kornack, D. R. & Rakic, P. (2001) *Science* **294,** 2127–2130.
13. Caceres, A., Binder, L. I., Payne, M. R., Bender, P., Rebhun, L. & Steward, O. (1984) *J. Neurosci.* **4,** 394–410.
14. Mullen, R. J., Buck, C. R. & Smith, A. M. (1992) *Development (Cambridge, U.K.)* **116,** 201–211.
15. Menezes, J. R. L. & Luskin, M. B. (1994) *J. Neurosci.* **14,** 5399–5416.
16. Minturn, J. E., Fryer, H. J., Geschwind, D. H. & Hockfield, S. (1995) *J. Neurosci.* **10,** 6757–6766.
17. Minturn, J. E., Geschwind, D. H., Fryer, H. J. & Hockfield, S. (1995) *J. Comp. Neurol.* **355,** 369–379.
18. Middleton, G., Piñón, L. G. P., Wyatt, S. & Davies, A. M. (1998) *J. Neurosci.* **18,** 3344–3350.
19. Suzuki, A. & Tsutomi, Y. (1998) *Brain Res.* **801,** 59–66.
20. Zhang, K. Z., Westberg, J. A., Höltä, E. & Anderson, L. C. (1996) *Proc. Natl. Acad. Sci. USA* **93,** 4504–4508.
21. Bernier, P. J. & Parent, A. (1998) *J. Neurosci.* **18,** 2486–2497.
22. Morshead, C. M. & van der Kooy, D. (1992) *J. Neurosci.* **12,** 249–256.
23. Pencea, V., Bingaman, K. D., Freedman, L. J. & Luskin, M. B. (2001) *Exp. Neurol.* **172,** 1–16.
24. Altman, J. & Das, G. D. (1965) *J. Comp. Neurol.* **124,** 319–336.
25. Feess-Higgins, A. & Larroche, J. C. (1987) *Development of the Human Foetal Brain: An Anatomical Atlas* (Masson, Paris).
26. Gould, E., Tanapat, P., McEwen, B. S., Flügge, G. & Fuchs, E. (1998) *Proc. Natl. Acad. Sci. USA* **95,** 3168–3171.
27. Kempermann, G., Kuhn, H. G. & Gage, F. H. (1997) *Nature (London)* **386,** 493–495.
28. Lois, C. & Alvarez-Buylla, A. (1993) *Proc. Natl. Acad. Sci. USA* **90,** 2074–2077.
29. Luskin, M. B. & McDermott, K. (1994) *Glia* **11,** 211–226.
30. Parent, A. (1996) *Carpenter's Human Neuroanatomy* (Williams & Wilkins, Baltimore), 9th Ed.
31. LeDoux, J. E. (2000) *Annu. Rev. Neurosci.* **23,** 155–184.
32. Wilensky, A. E., Schafe, G. E. & LeDoux, J. E. (2000) *J. Neurosci.* **15,** 7059–7066.
33. Martin, S. J., Grimwood, P. D. & Morris, R. G. M. (2000) *Annu. Rev. Neurosci.* **23,** 649–711.